13th World Conference on Earthquake Engineering
Vancouver, B.C., Canada
August 1-6, 2004
Paper No. 245

SIMPLIFIED SEISMIC ANALYSIS OF WOODFRAME STRUCTURES

Bryan FOLZ[1] and Andre FILIATRAULT[2]

SUMMARY

A simple numerical model to predict the dynamic characteristics, quasi-static pushover and seismic response of woodframe buildings is presented. In this model, the building structure is composed of two primary components: rigid horizontal diaphragms and nonlinear lateral load resisting shear wall elements. The actual three-dimensional building is degenerated into a two-dimensional planar model using zero-height shear spring elements connected between adjacent diaphragms or the foundation. The hysteretic behavior of each wood shear wall in the building can be characterized using an associated numerical model that predicts the walls load-displacement response under general quasi-static cyclic loading. In turn, in this model, the hysteretic behavior of each shear wall is represented by an equivalent nonlinear shear spring element. With this simple structural model, the response of the building is defined in terms of only three-degrees-of-freedom per floor. This numerical model has been incorporated into the computer program SAWS - Seismic Analysis of Woodframe Structures. The predictive capabilities of the SAWS model are compared with shake table tests performed on a full-scale two-storey woodframe house as part of the recently completed CUREE-Caltech Woodframe Project. It is shown in this study that the SAWS computer program provides reasonably accurate estimates of the dynamic characteristics, quasi-static pushover and seismic response of this test structure. Furthermore, the SAWS program requires a minimum amount of data input and provides a fast computational turn-around time to analyze a given structure. As a result, this simple numerical model may be a useful structural analysis tool for practicing engineers and researchers.

INTRODUCTION

Light-frame residential wood buildings are by far the most common structures constructed in North America. These building systems range in size from small, single-story dwellings to large, multi-level, multiple-occupancy condominiums and apartments. The primary structural components of these building are typically horizontal floor diaphragms, horizontal or sloped roof diaphragms and vertical shear walls. Each of these structural elements is generally composed of sawn lumber framing members attached to sheathing panels using dowel connectors, such as nails, and/or adhesives. Typically, these elements are interconnected through nailed connections to make up the overall structural system for the building. With

[1] Faculty, British Columbia Institute of Technology, Burnaby, Canada. Email: bfolz@bcit.ca
[2] Deputy Director of the Multidisciplinary Center for Earthquake Engineering Research and Professor of Structural Engineering, State University of New York, Buffalo, NY, USA.
Email: filiatrault@mceermail.buffalo.edu

this type of construction the resulting building typically has a high degree of structural redundancy. In addition, the inelastic response of the building under severe lateral loading conditions may display significant degradation in strength and stiffness. These complicating factors have contributed to paucity in dedicated three-dimensional structural analysis models for woodframe building [1]. This is in contrast to the abundance of static and dynamic structural analysis tools available to evaluate the response of building frames composed of other construction materials such as structural steel or reinforced concrete.

In the modeling of woodframe structures, it has been noted that if all of the structural details within a woodframe building is captured within a finite element model, the required computational overhead can overwhelm practical computing capability [2]. Therefore, model reduction techniques must be implemented to produce usable numerical simulations. Another maxim at work is: the more detailed the model, the greater the dependency on test data to calibrate the model. Unfortunately, the requisite test data is not always readily available.

With these considerations in mind, this paper presents a simple and versatile numerical model that predicts the dynamic characteristics, quasi-static pushover and seismic response of light-frame wood buildings. The basic modeling approach is to degenerate the actual three-dimensional building into a two-dimensional planar model composed of zero-height shear wall spring elements connecting the floor and roof diaphragms together or to the foundation. All diaphragms in the building model are assumed to have infinite in-plane stiffness. Using this simple modeling approach, the response of the building is defined in terms of only three-degrees-of-freedom (3-DOF) per floor. Each shear wall spring element is calibrated to reflect the strength and stiffness degrading hysteretic characteristics of the associated shear wall it is modeling in the structure. Requisite test data is limited to that necessary to characterize the behavior of the shear walls. This three-dimensional numerical model has been incorporated into the computer program SAWS - Seismic Analysis of Woodframe Structures [3]. This paper provides an overview of the model formulation. As well, the predictive capabilities of this model are compared with experimental results from recent shake table tests performed on a full-scale two-story wood frame house. It is shown that the model predictions are in good agreement with the test results with respect to both the dynamic characteristics and seismic response of the building structure.

MODEL FORMULATION

Structural Configuration of the Building Model

For illustrative purposes, the structural configuration of a typical woodframe building is discussed in terms of the simplified single-story building layout shown in Fig. 1a. The main structural elements that compose the building are: the exterior and/or interior shear walls, the interior partition walls and the floor and/or roof diaphragms. The building structure is assumed to be attached to a rigid foundation. In the modeling of the structure, it is assumed that both the floor and roof elements have sufficiently high in-plane stiffness to be considered as rigid elements. This is expected to be a reasonable assumption for typically constructed diaphragms with a planar aspect ratio of the order of 2:1, as supported by experimental results from full-scale diaphragms tests [4]. Further to this, it is assumed that an equivalent horizontal diaphragm can adequately model a sloping roof. As a final modeling step, the three-dimensional building structure is degenerated to a planar model by assigning zero-height to all of the shear wall elements that connect the horizontal diaphragms to the foundation. Each shear wall in the building structure is, in turn, represented by an equivalent single-degree-of-freedom (SDOF) shear element via a calibration procedure discussed in a subsequent section. Applying this overall modeling approach to the building structure illustrated in Fig. 1a produces the simplified building model shown in Fig. 1b.

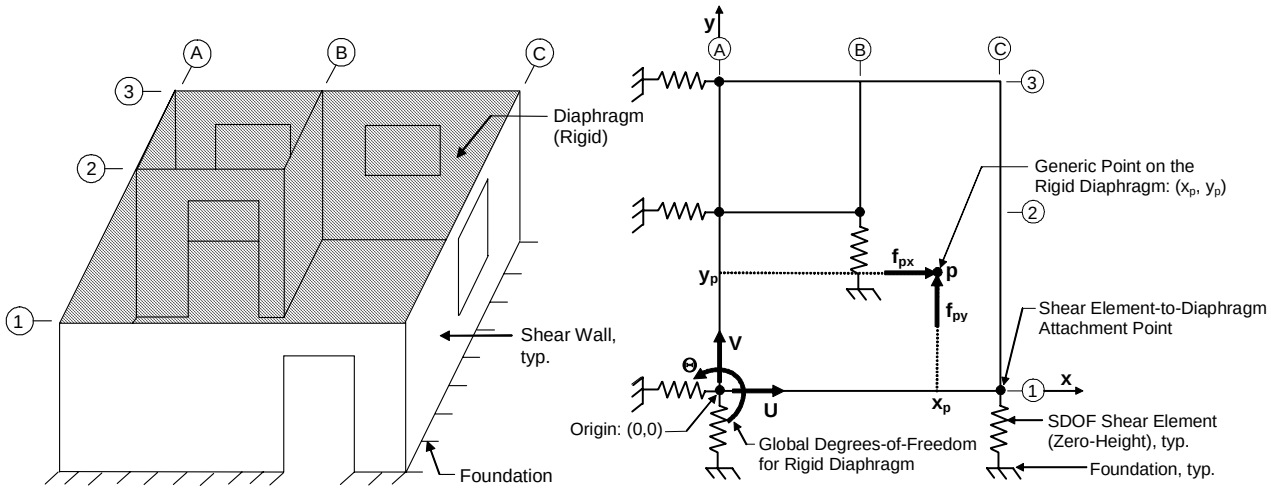

(a) (b)

Figure 1: (a) Components of a single-storey woodframe structure. (b) Model of the single-storey woodframe structure.

It is noted that this degenerated planar model does not capture the overturning and flexural response of a building. However, this is not viewed as a significant limitation of this model for its intended application. Most woodframe buildings are low-rise structures so that overturning is not typically significant and the deformation mode is primarily one of shear.

Kinematic Assumptions for the Building Model

To analyze the simplified building model presented in Fig. 1b, a global rectangular coordinate system is prescribed as shown so that the entire building structure is contained within the first quadrant. The global degrees-of-freedom of each diaphragm are then assigned at the origin of the coordinate system. Under the assumption that each diaphragm is rigid, only three global degrees-of-freedom are required to completely describe its rigid body motion: two translations U and V and one rotation Θ. Under a general displaced state of the diaphragm specified by the values of U, V and Θ, the resulting linearized displacement of any point p on the diaphragm can be expressed in matrix form as:

$$\begin{Bmatrix} u_p \\ v_p \\ \theta_p \end{Bmatrix} = \begin{bmatrix} 1 & 0 & -y_p \\ 0 & 1 & x_p \\ 0 & 0 & 1 \end{bmatrix} \begin{Bmatrix} U \\ V \\ \Theta \end{Bmatrix} = \mathbf{\Lambda D} \tag{1}$$

where $\mathbf{\Lambda}$ is a transformation matrix and $\mathbf{D} = [U, V, \Theta]^T$ is the global displacement vector.

Load Vector and Stiffness Matrix Formulation

Consider the application of external forces f_{px} and f_{py} located at any point p on the diaphragm, with the line of action of f_{px} parallel to the x-axis and the line of action of f_{py} parallel to the y-axis, as shown in Fig. 1b. These forces are statically equivalent to the following system of forces applied at the origin:

$$\begin{Bmatrix} F_U \\ F_V \\ M_\Theta \end{Bmatrix} = \begin{bmatrix} 1 & 0 & 0 \\ 0 & 1 & 0 \\ -y_p & x_p & 1 \end{bmatrix} \begin{Bmatrix} f_{px} \\ f_{py} \\ 0 \end{Bmatrix} = \mathbf{\Lambda}^T \begin{Bmatrix} f_{px} \\ f_{py} \\ 0 \end{Bmatrix} \tag{2}$$

where $\mathbf{F} = [F_U, F_V, M_\Theta]^T$ is the global force vector that is conjugate to the global displacement vector **D**. The force transformation relationship given by Eq. (2) can be used to represent all types of loads applied to the diaphragm including inertia forces as well as the restoring forces developed in the SDOF shear elements.

For a given building structure let N_x and N_y denote the number of SDOF shear elements parallel to the x-axis and y-axis, respectively. For the example building model shown in Fig. 1b $N_x = N_y = 3$. For the i-th SDOF shear element aligned parallel to the x-axis, let k_{ix} denote its in-plane stiffness. Similarly, let k_{jy} denote the in-plane stiffness of the j-th SDOF shear element aligned parallel to the y-axis. Out-of-plane stiffness in all shear elements is assumed to be zero. This assumption is expected to be reasonable for an isolated shear wall, however it also implies that intersecting shear walls behave independently of each other, which typically is not the case.

The force developed in a SDOF shear element resulting from a displacement of the diaphragm can be related to the global forces in the structure through Eq. (2). Also, the displacement of the SDOF shear element can be related to the global displacement of the diaphragm through Eq. (1). Applying and combining these two steps over all SDOF shear elements in the building model results in the generation of the global stiffness matrix **K**:

$$\mathbf{K} = \sum_{ix=1}^{Nx} \left(\mathbf{\Lambda}_{ix}^T \mathbf{K}_{ix} \mathbf{\Lambda}_{ix} \right) + \sum_{jy=1}^{Ny} \left(\mathbf{\Lambda}_{jy}^T \mathbf{K}_{jy} \mathbf{\Lambda}_{jy} \right) \tag{3}$$

where $\mathbf{K}_{ix}$ and $\mathbf{K}_{jy}$ are given, respectively, by:

$$\mathbf{K}_{ix} = \begin{bmatrix} k_{ix} & 0 & 0 \\ 0 & 0 & 0 \\ 0 & 0 & 0 \end{bmatrix} \text{ and } \mathbf{K}_{jy} = \begin{bmatrix} 0 & 0 & 0 \\ 0 & k_{jy} & 0 \\ 0 & 0 & 0 \end{bmatrix} \tag{4a,b}$$

As presented, $\mathbf{K}_{ix}$ and $\mathbf{K}_{jy}$ apply to a 3-DOF building model such as shown in Fig. 1b. In Eq. (3), the coordinates in the transformation matrices $\mathbf{\Lambda}_{ix}$ and $\mathbf{\Lambda}_{jy}$ identify the point of attachment of the SDOF shear element to the diaphragm. Extension of the formulation of the global force vector and stiffness matrix to multi-story building structures is straightforward.

For the global stiffness matrix **K** presented above, it is important to note that the contributing stiffness of each SDOF shear element is, for the problem at hand, load (or displacement) history dependent. A general characterization of the hysteretic response of the SDOF shear elements is presented in the subsequent section.

SDOF Hysteretic Model of Wood Shear Walls

The force-deformation response of a wood shear wall with dowel-type sheathing-to-framing connectors is nonlinear under monotonic loading and additionally exhibits pinched hysteretic behavior with strength and stiffness degradation under general cyclic loading. It is well recognized that the global force-deformation response of a wood shear wall is qualitatively very similar to that of the individual sheathing-to-framing connectors used in the construction of the wall [5].

Consequently, when properly calibrated, the same hysteretic model used for sheathing-to-framing connectors can be applied to model the global cyclic response of a shear wall. The authors have previously developed a general hysteretic model for sheathing-to-framing connectors, which is defined in terms of a number of path following rules to reproduce the response of a connector under arbitrary cyclic

loading [5]. This same hysteretic model is adopted herein to model the global cyclic response of a wood shear wall.

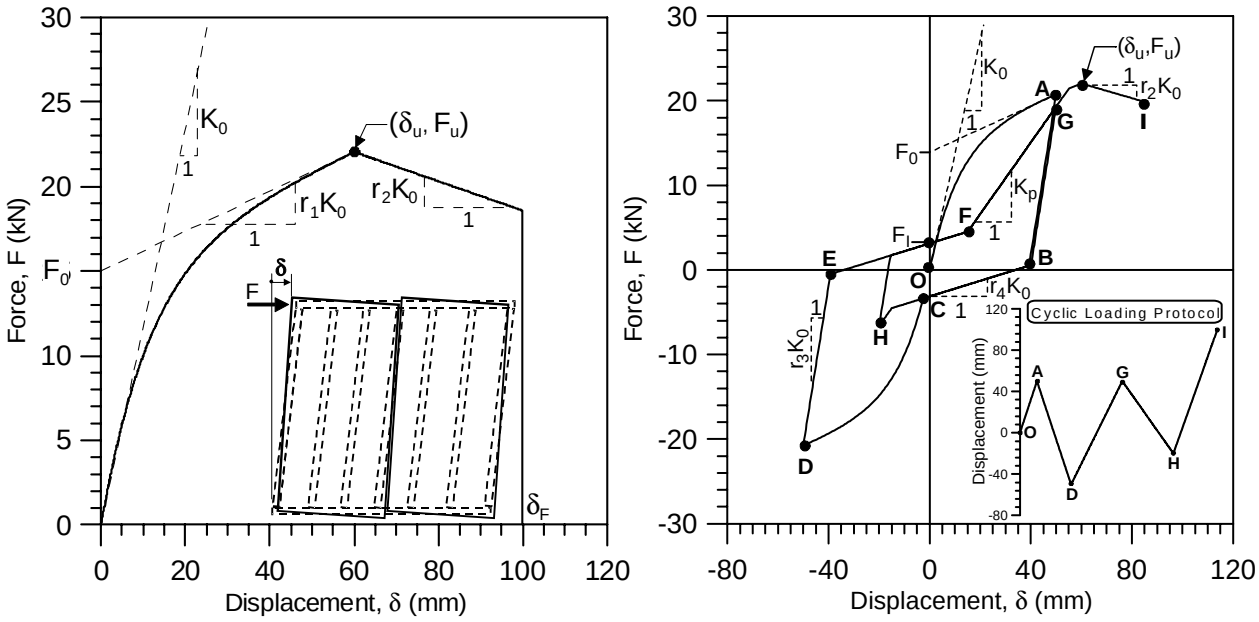

(a) (b)

Figure 2: Force-displacement response of a wood shear wall under: (a) monotonic loading and (b) cyclic loading. The hysteretic model is fitted to test data for a 2.4 m by 2.4 m shear wall with 9.5 mm thick OSB panels [8].

Figure 2a shows the assumed force-deformation behavior of a wood shear wall under monotonic loading to failure. The monotonic racking response, in terms of top-of-wall force F and displacement δ (see the insert in Fig. 2a) is modeled by the following nonlinear relationship:

$$F = \begin{cases} \operatorname{sgn}(\delta)\cdot\left(F_0 + r_1 K_0 |\delta|\right)\cdot\left[1-\exp\left(-K_0|\delta|/F_0\right)\right], & |\delta| \le |\delta_u| \\ \operatorname{sgn}(\delta)\cdot F_u + r_2 K_0\left[\delta - \operatorname{sgn}(\delta)\cdot\delta_u\right], & |\delta_u| < |\delta| \le |\delta_F| \\ 0, & |\delta| > |\delta_F| \end{cases} \tag{5}$$

This force-deformation model is characterized by six physically identifiable parameters: F_0, K_0, r_1, r_2, δ_u and δ_F. Phenomenologically, Eq. (5) captures the crushing of the framing members and sheathing along with yielding of the connectors. Beyond the displacement δ_u, which is associated with the ultimate load F_u, the load-carrying capacity is reduced. Failure of the wall under monotonic loading occurs at the displacement δ_F.

Next, consider the force-deformation response of a shear wall under the cyclic loading shown as an insert in Fig. 2b. The basic path following rules which define the hysteretic model are identified and briefly discussed. In Fig. 2b, force-deformation paths OA and CD follow the monotonic envelope curve as expressed by Eq. (5). All other paths are assumed to exhibit a linear relationship between force and deformation. Unloading off the envelope curve follows a path such as AB with stiffness r_3K_0. Here the wall unloads elastically. Under continued unloading, the response moves onto path BC that is characterized by a reduced stiffness r_4K_0. The very low stiffness along this path exemplifies the pinched hysteretic response displayed by wood shear walls under cyclic loading. This behavior occurs because of

the previously induced crushing of the framing members and sheathing panels around the connectors (in this case as the wall followed the path OA). Loading in the opposite direction for the first time forces the response onto the envelope curve CD. Unloading off this curve is assumed elastic along path DE, followed by a pinched response along path EF, which passes through the zero-displacement intercept F_I, with slope r_4K_0. Continued re-loading follows path FG with degrading stiffness K_p, as given by

$$K_p = K_0\left(\frac{\delta_0}{\delta_{max}}\right)^{\alpha} \tag{6}$$

with $\delta_0 = (F_0/K_0)$ and α a hysteretic model parameter which determines the degree of stiffness degradation. Note from Eq. (6) that K_p is a function of the previous loading history through the last unloading displacement δ_{un} off the envelope curve (corresponding to point A in Fig. 2b), so that

$$\delta_{max} = \beta\delta_{un} \tag{7}$$

where β is another hysteretic model parameter. A consequence of this stiffness degradation is that it also produces strength degradation in the response. If on another cycle the shear wall is displaced to δ_{un}, then the corresponding force will be less than F_{un} which was previously achieved. This strength degradation is shown in Fig. 2b by comparing the force levels obtained at points A and G. Also, with this model under continued cycling to the same displacement level, the force and energy dissipated per cycle is assumed to stabilize beyond the second loading cycle.

In total, 10 parameters are required to define this hysteretic model. To obtain these parameters for a particular wood shear wall, an analysis tool such as the CASHEW (Cyclic Analysis of SHEar Walls) computer program [6] can be employed. The CASHEW program assumes that a shear wall is composed of pin-connected rigid framing members, elastic shear deformable sheathing members and nonlinear sheathing-to-framing connectors that follow the same hysteretic model described above. With the CASHEW program, a given wall is first subjected to the CUREE-Caltech Testing Protocol [7], after which a fitting procedure extracts the parameters to represent the wall response by an equivalent SDOF shear wall spring element. This model reduction approach has been successfully evaluated against experimental tests. As an example, the force-deformation response shown in Fig. 2b was produced using the parameters obtained from the CASHEW program for a 2.4 m by 2.4 m shear wall with 9.5 mm thick oriented strand board (OSB) sheathing panels that was also tested cyclically and under an earthquake ground motion on a shake table [8]. Comparison between the experimental results and the predicted responses of the reduced shear wall model showed good agreement [5].

In recent years, there has been a proliferation of cyclic tests performed on full-scale wood framed shear walls. The resulting database of experimental results can be used to specify equivalent SDOF shear spring elements for each of the walls that have been tested. This approach has been utilized by the authors to calibrate shear spring elements to model shear walls sheathed with stucco and gypsum wall board [3].

Dynamic Analysis

The governing equations of motion for a three-dimensional structure when subjected to an earthquake ground motion are given by:

$$\mathbf{M}\ddot{\mathbf{D}}(t) + \mathbf{C}\dot{\mathbf{D}}(t) + \mathbf{F}_{sw}(\mathbf{D}(t)) = -\mathbf{M}\mathbf{r}\ddot{x}_g(t) \tag{8}$$

where $\mathbf{M}$ is the global mass matrix; $\mathbf{C}$ is the global viscous damping matrix; $\mathbf{F}_{sw}(t)$ is the global restoring force vector generated by all of shear wall elements in the structure; $\ddot{\mathbf{D}}(t)$, $\dot{\mathbf{D}}(t)$ and $\mathbf{D}(t)$ are, respectively, the global acceleration, velocity and displacement vectors relative to the ground; $\ddot{x}_g(t)$ is the ground acceleration and $\mathbf{r}$ is a vector coupling the ground motion input with the global degrees-of-freedom

excited by that motion. The right hand side of Eq. (8) must be replaced by the more general expression $-\mathbf{M}\left[\mathbf{r}_U \ddot{x}_{gU}(t) + \mathbf{r}_V \ddot{x}_{gV}(t)\right]$ for the case of bi-directional ground accelerations $\ddot{x}_{gU}(t)$ and $\ddot{x}_{gV}(t)$ applied parallel to the x-axis and y-axis, respectively.

The global mass matrix **M**, given in Eq. (8), can be obtained through consideration of dynamic equilibrium and application of D'Alembert's Principle. With reference to Fig. 1b, the global mass matrix for a single story structure is given by:

$$\mathbf{M} = \begin{bmatrix} m & 0 & -my_c \\ 0 & m & mx_c \\ -my_c & mx_c & I_0 + m(x_c^2 + y_c^2) \end{bmatrix} \tag{9}$$

where m is the mass of the diaphragm, (x_c, y_c) are the coordinates of its center of mass from an absolute reference and I_0 is the mass moment of inertia about the center of mass. As presented, Eq. (9) only represents the contributing mass from the diaphragm; mass associated with each shear wall can be represented by a discrete mass that includes rotatory inertia and added appropriately to Eq. (9).

The global viscous damping matrix **C,** given in Eq. (8), accounts for all supplemental energy dissipating mechanisms in the structure other than the hysteretic damping produced in the shear wall elements. In this study a Rayleigh damping model is assumed.

To advance the solution of Eq. (9), from time t to t+Δt, the equations of motion are rewritten in incremental form:

$$\mathbf{M}\Delta\ddot{\mathbf{D}} + \mathbf{C}\Delta\dot{\mathbf{D}} + \Delta\mathbf{F}_{sw} = -\mathbf{M}\mathbf{r}\Delta\ddot{x}_g(t) \tag{10}$$

with $\Delta(\cdot) = (\cdot)_{t+\Delta t} - (\cdot)_t$. Within each time step, the structural response is assumed linear. As a consequence, the increment in the global restoring force is given by:

$$\Delta\mathbf{F}_{sw} = \mathbf{K}_T \Delta\mathbf{D} \tag{11}$$

where $\mathbf{K}_T$ is the global tangent stiffness matrix given by Eq. (3) and evaluated at time t. Newmark's Method, utilizing constant average acceleration within a time step, is used to integrate Eq. (10) over the time domain.

As presented, this incremental solution strategy does not guarantee that equilibrium is achieved at the end of each time step. To minimize the accumulation of error over time, the relative acceleration at time t + Δt is determined by enforcing dynamic equilibrium of Eq. (8) at the end of each time step. In turn, this adjusted value of acceleration is used in the next time step of the incremental solution strategy.

Also, energy balance calculations are performed at the end of each time step to monitor the accuracy of this solution strategy as well as to assess the energy absorption capacity of the shear wall elements of the structure. The process of integrating the equations of motion is generally aborted if an energy balance is not satisfied within a specified tolerance.

Pushover Analysis

The governing equations of motion for a three-dimensional structure when subjected to a general dynamic force excitation are given by:

$$\mathbf{M}\ddot{\mathbf{D}}(t) + \mathbf{C}\dot{\mathbf{D}}(t) + \mathbf{F}_{sw}\left(\mathbf{D}(t)\right) = \mathbf{P}(t) \tag{12}$$

where Eq. (12) is identical to Eq. (8) except that the right- hand side of the equation has been replaced by the global applied forcing function **P**(t). In order to perform a uni-directional quasi-static pushover analysis parallel to the x-axis or y-axis, using Eq. (12), **P**(t) is decomposed as follows:

$$\mathbf{P}(t) = p(t) \cdot \mathbf{F} \tag{13}$$

with p(t) representing the temporal variation of a slowly varying, monotonically increasing, applied pushover load, while **F** determines the distribution of nodal forces acting on the structure. The time varying load p(t) takes the form:

$$p(t) = \frac{1}{2}\left[1 - \cos\left(\frac{\pi t}{T_p}\right)\right] \cdot P_{max} \qquad 0 \le t \le T_p \tag{14}$$

where P_{max} represents the magnitude of the maximum lateral load applied to the structure and T_p is the duration of the applied loading. To minimize the contribution from inertia and damping effects in Eq. (12), the duration of loading T_p is set to one hundred times the computed fundamental elastic period of the structure.

The distribution of the lateral loading applied at the global degrees-of-freedom is determined through **F**. First off, **F** represents nodal loads equivalent to pushover loads applied at the center of mass of each floor of the structure. Three options on the distribution of loading over the height of the structure are considered in this analysis: a uniform distribution, an inverted triangular distribution and a modal adaptive distribution [3]. In general, specification of an appropriate lateral load distribution is a weak point in the pushover methodology. At least being able to utilize the three different distribution noted above can help determine the response sensitivity of a given structure to applied lateral loadings.

SAWS Computer Program

The model formulation presented above has been incorporated into the computer program SAWS – Seismic Analysis of Woodframe Structures [3]. This computer program has analysis options to predict the dynamic characteristics, quasi-static pushover and seismic response of light-frame wood buildings.

MODEL VERFICATION

Description of the Verification Test Structure

In seeking to validate the SAWS numerical model, it must be noted at the outset that very few tests have been conducted in North America on full-scale light-frame wood buildings. As part of the CUREE-Caltech Woodframe Project a simplified full-scale two-story single-family house was tested on a uniaxial earthquake facility [9]. This extensive experimental study considered 10 different construction phases of the test structure. Only the fully engineered Phase 9 test structure, as described below, will be used in the verification study of the SAWS model.

Figure 3 shows plan and elevation views of the test structure along with the identification of the major structural components used in its construction. The Phase 9 test structure included only the bare wood framing; interior and exterior wall finishes were not included nor were door and window details.

The design of the Phase 9 test structure was based on the engineering provisions of the 1994 edition of the Uniform Building Code [10] for a seismic zone 4 and common design practices in California. The design assumes a force-reduction factor R_w of 8, for a lateral load-resisting system consisting light-frame wood shear walls. The seismic weight of the structure was 110 kN and the period of vibration estimated by the code was 0.18 seconds. The resulting design base shear in the shaking (north-south) direction was 15 kN. The ultimate base shear capacity of the test structure was estimated to be 75 kN, according to the FEMA 273 guidelines [11].

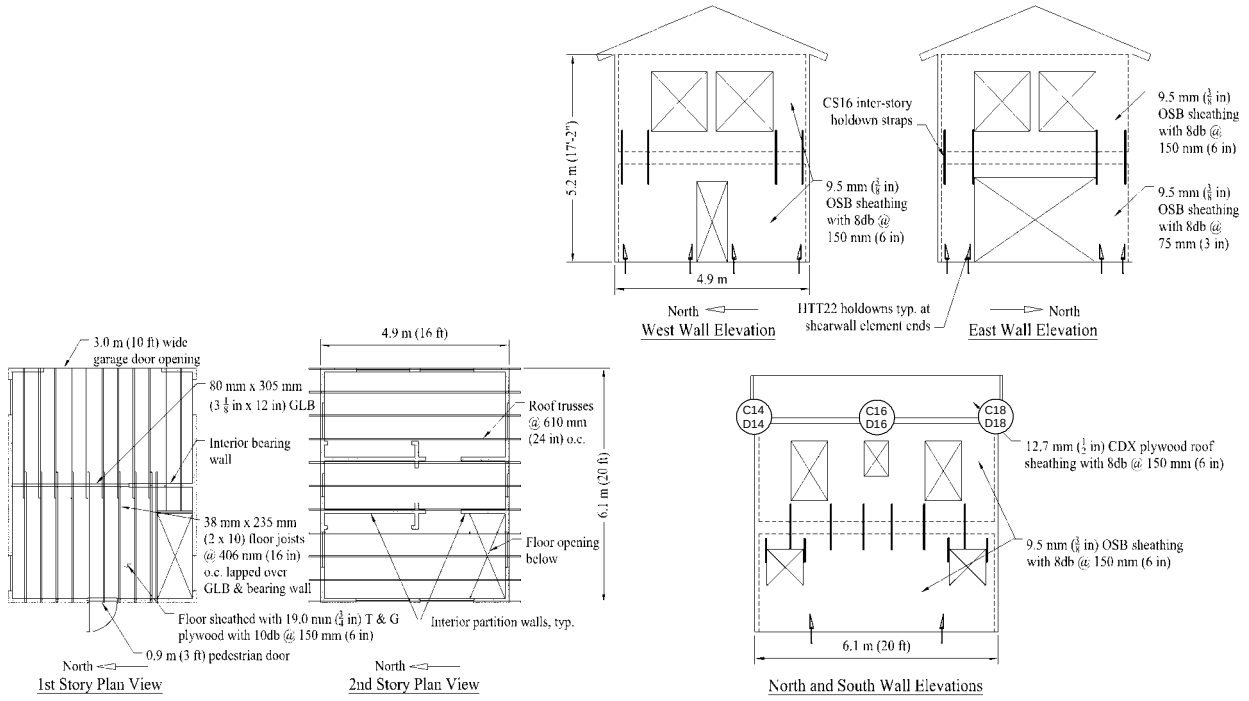

Figure 3: Plan and elevation views of the test structure, with major structural components identified.

During Phase 9, the test structure was subjected to an extensive series of shake table motions, which included harmonic, white noise and seismic ground motions. The white noise was used to determine frequencies and mode shapes of the structure under low amplitude vibrations. The harmonic input at the natural frequency of the structure was used to ascertain its damping characteristics. The seismic ground motions were used to determine the inelastic response of the structure under increasing intensities of shaking. Five levels of seismic tests were performed on the test structure. The input ground motion for seismic test levels 1 to 4 represents a scaling of the 1994 Northridge Earthquake recorded at Canoga Park, as shown in Fig. 4. The input ground motion for seismic test level 5 represents the unscaled 1994 Northridge Earthquake recorded at Rinaldi, also shown in Fig 4. Seismic test level 4 represents a ground motion with a hazard level of 10% probability of exceedance in 50 years. Seismic test level 5 represents a ground motion with a hazard level of 2% probability of exceedance in 50 years. As part of the test program, one seismic test was repeated once the maximum transient inter-story wall drift exceeded 0.5% of its height. For Phase 9 this occurred at level 3. Figure 4 presents the complete sequence of acceleration records applied to the Phase 9 shake table test structure. Over Phase 9 the test structure was subjected, in turn, to each one of these ground motions without any repair or modification to the structure.

The test structure was monitored with nearly three hundred digital instruments to measure forces, displacements and accelerations in the structure during the shake table tests. For the evaluation of the SAWS model predictions, response quantities of interest will be limited to relative displacement and absolute acceleration time-histories at the roof level. Data acquisition sensors to measure displacement (C14, C16 and C18) and acceleration (D14, D16 and D18) were placed at roof level along the east wall, center-line and west wall of the structure, as shown in Fig. 3.

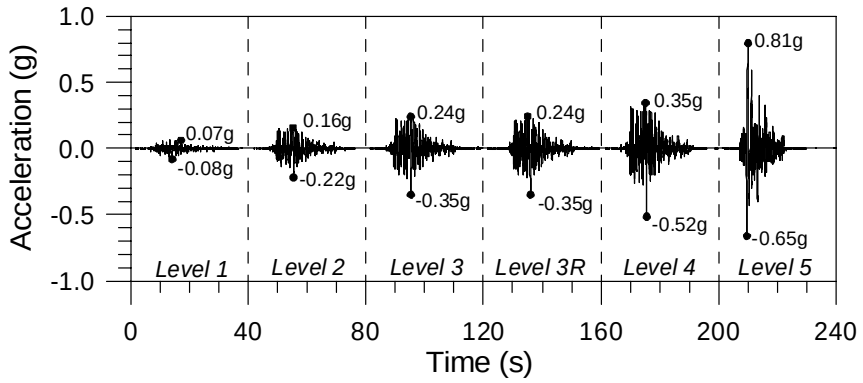

Figure 4: Sequence of acceleration records applied to the shake-table test structure.

SAWS Model of the Test Structure

The SAWS model for the test structure is schematically shown in Fig. 5. It is composed of eight zero-height shear wall spring elements and two rigid diaphragms; one for the second floor and one at the roof level. The force-deformation response of each shear wall spring element requires the specification of ten hysteretic parameters, as discussed previously. These parameters were determined using the analysis program CASHEW - Cyclic Analysis of SHEar Walls [6]. As an example from this analysis step, Fig. 6 shows the CASHEW model predictions of the cyclic response of the first and second level east shear walls of the test structure. As determined by the CASHEW program, the calibrated hysteretic parameters required to describe the cyclic response of the eight Phase 9 shear walls are given Table 1. In Fig. 5 and Table 1, the eight shear spring elements have been identified using the notation S_{xi} and S_{yi}, with i =1, ..4 and the subscript x and y indicating that an element is aligned either along the x or y axis.

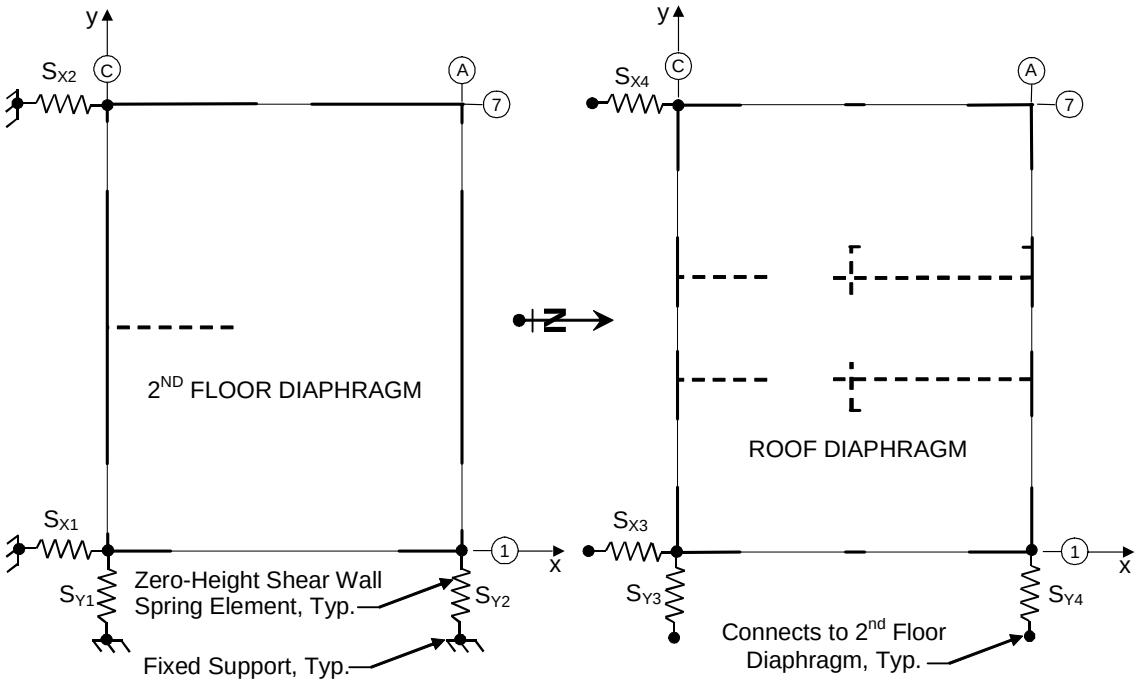

Figure 5: SAWS model of the test structure.

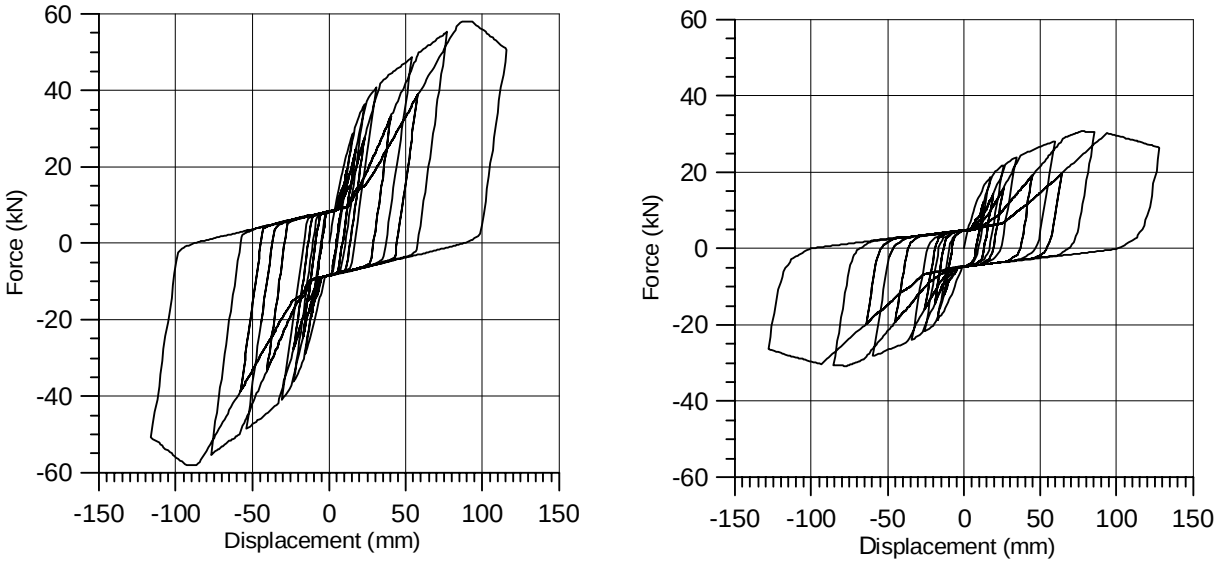

(a) 1st floor east shear wall (b) 2nd level east shear wall

Figure 6: CASHEW predictions of the cyclic response of the test structure shear walls.

Table 1: Hysteretic parameters for the shear wall spring elements in the test structure.

Spring Element	K_0 (kN/mm)	r_1	r_2	r_3	r_4	F_0 (kN)	F_1 (kN)	Δ_u (mm)	α	β
S_{X1} Level 1 East Wall	2.93	0.083	-0.088	1.00	0.03	36.6	8.36	87.3	0.79	1.07
S_{X2} Level 1 West Wall	3.89	0.064	-0.056	1.07	0.03	36.7	8.82	57.8	0.87	1.11
S_{Y1} Level 1 South Wall	5.69	0.065	-0.074	1.10	0.03	48.4	10.8	60.6	0.81	1.09
S_{Y2} Level 1 North Wall	5.69	0.065	-0.074	1.10	0.03	48.4	10.8	60.6	0.81	1.09
S_{X3} Level 2 East Wall	2.10	0.069	-0.038	1.16	0.02	19.6	4.76	76.8	0.77	1.10
S_{X4} Level 2 West Wall	2.10	0.069	-0.038	1.16	0.02	19.6	4.76	76.8	0.77	1.10
S_{Y3} Level 2 South Wall	3.35	0.054	-0.060	1.10	0.03	35.3	12.9	73.9	0.84	1.09
S_{Y4} Level 2 North Wall	3.35	0.054	-0.060	1.10	0.03	35.3	12.9	73.9	0.84	1.09

SAWS Model Predictions

Dynamic and Seismic Analysis of the Test Structure

The SAWS model of the Phase 9 shake table test structure predicted a fundamental frequency of 3.28 Hz. This prediction is based on assigned seismic weights of 62 kN to the second floor diaphragm and 48 kN to the roof diaphragm. At the start of Phase 9 testing, the experimentally measured fundamental frequency was 3.96 Hz [9]. The SAWS model under predicts the experimental result by 17%. Potential sources for this difference are the inherent simplicity of the SAWS model and the CASHEW predictions of the initial stiffness of each shear wall element.

Figures 7 and 8 present the SAWS model predictions of the relative displacement time-histories along the centerline of the test structure at roof level for level 4 and 5 testing along with the corresponding experimental results. These relative displacement measurements correspond to sensor C16, as shown in Fig. 3. The SAWS model predictions are based on an assigned equivalent viscous damping of 1% of critical in the first and second elastic modes of vibration. It is assumed that under the strong motion portions of shaking of levels 4 and 5, that damping in the structure can largely be accounted for through the hysteretic response of the shear wall spring elements. As a consequence, the viscous damping is set to a low value. This modeling approach is consistent with what has been suggested by other research work [5]. Experimentally, the equivalent viscous damping for the test structure was calculated to be 4.2% of critical under small amplitude excitation.

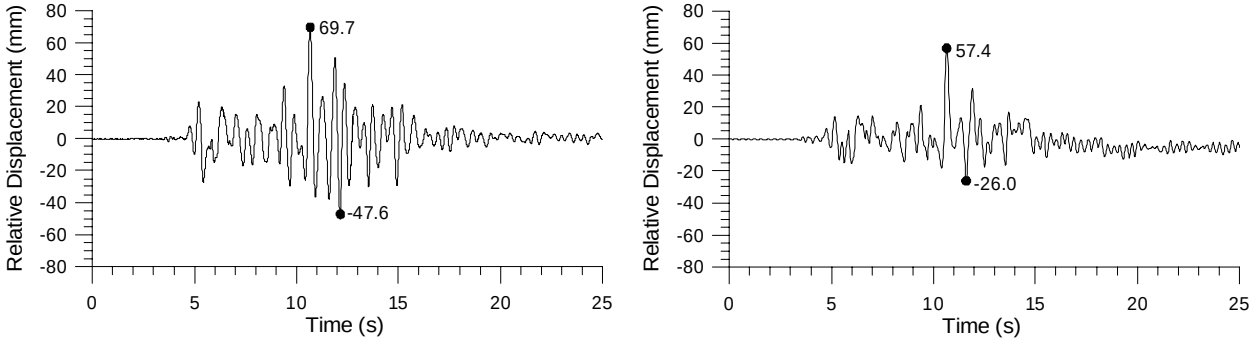

(a) Experimental Result (b) SAWS prediction

Figure 7: Level 4 relative displacement time histories at Sensor C16: (a) experimental result and (b) SAWS prediction.

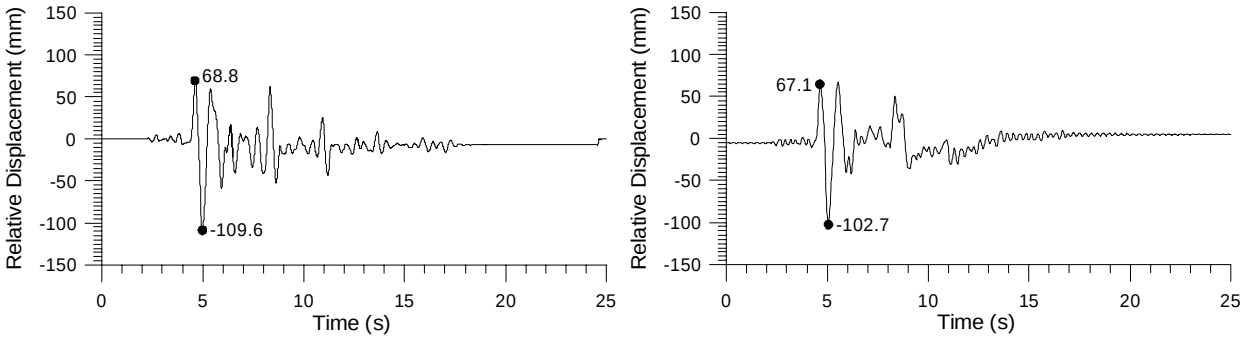

(a) Experimental Result (b) SAWS prediction

Figure 8: Level 5 relative displacement time histories at Sensor C16: (a) experimental result and (b) SAWS prediction.

With respect to maximum response values, over levels 4 and 5, the maximum relative displacement at sensor location C16 estimated by the SAWS model under predicts the experimental values by 17.6% and 6.3%, respectively. Table 2 provides a complete listing of the maximum response values predicted by the SAWS model and obtained experimentally for all of the sensor locations shown in Fig. 3. Comparing the maximum relative displacement results given in Table 2, the differences in the numerical predictions and the experimental values can, in part, be attributed to the SAWS model not fully capturing the torsional response of the Phase 9 test structure and also the model's inability to account for the in-plane deformation in the roof diaphragm. Over test levels 4 and 5, the maximum torsional response resulted in a difference in relative displacement between the east and west walls of 5.2 mm and 11.7 mm, respectively.

Also for levels 4 and 5, the maximum roof diaphragm deformations were 5.8 mm and 7.1 mm, respectively.

Table 2: Comparison of maximum relative displacement and maximum absolute acceleration response quantities from SAWS predictions and experimental results.

	Sensor Locations		
	C14 & D14	**C16 & D16**	**C18 & D18**
Level 4 – Maximum Relative Displacement (mm)			
SAWS Model	57.3	57.4	57.5
Test Result	61.3	69.7	66.5
% Error	*-6.5*	*-17.6*	*-13.5*
Level 4 – Maximum Absolute Acceleration (g)			
SAWS Model	0.99	0.99	1.05
Test Result	1.16	1.21	1.13
% Error	*-14.7*	*-19.6*	*-7.01*
Level 5 – Maximum Relative Displacement (mm)			
SAWS Model	102.8	102.7	102.6
Test Result	96.7	109.6	108.4
% Error	*6.3*	*-6.3*	*5.4*
Level 5 – Maximum Absolute Acceleration (g)			
SAWS Model	1.35	1.23	1.18
Test Result	1.27	1.36	1.39
% Error	*6.3*	*-9.6*	*-15.1*

All of the dynamic time-history results were produced by the SAWS computer program using a time integration step of 0.001 sec. In order to properly capture the evolution of damage to the structure over the Phase 9 testing regime, the SAWS computer program was run using the train of shake table acceleration input records from level 3 to 5 (see Fig. 4). The experimental results showed that very little damage occurred to the Phase 9 structure under level 1 and 2 testing. The numerical analysis was performed with a specified tolerance of 5% on the error in the energy balance applied to the equations of motion. The computational time required to perform a given level of analysis on the Phase 9 test structure using the SAWS program on a modern desktop computer was of the order of only 10 seconds. This fast computational turn-around time is attributable to the fact the SAWS computer program models the two-story shake table test structure using only six degrees-of-freedom.

Pushover Analysis of the Test Structure

A static pushover test was not performed on the shake table structure. However, from the seismic test data from Phase 9, a capacity spectrum was generated as shown in Fig. 9. The capacity spectrum is a plot of the maximum base shear (obtained as the sum of the floor and roof inertia forces) versus the corresponding peak roof relative displacement (measured at sensor location C16) for each test level [9].

With the capacity spectrum, the computed base shear represents the force induced in the foundation of the test structure including the nonlinear restoring force and viscous damping force. In a static pushover, only the nonlinear restoring force is activated since the resulting velocity of the structure is negligible during such a test. Thus, it is to be expected that the maximum base shear predicted by a static pushover analysis would be less than that estimated by a capacity spectrum. Figure 9 shows the SAWS model predictions from three static pushover analyses, corresponding to lateral load distributions that are uniform, triangular and modal adaptive. These three results are in relatively close agreement with each other and predict a

maximum base shear for the test structure of approximately 100 kN. For comparative purposes, estimates of design and ultimate maximum base shears are also shown in Fig. 9.

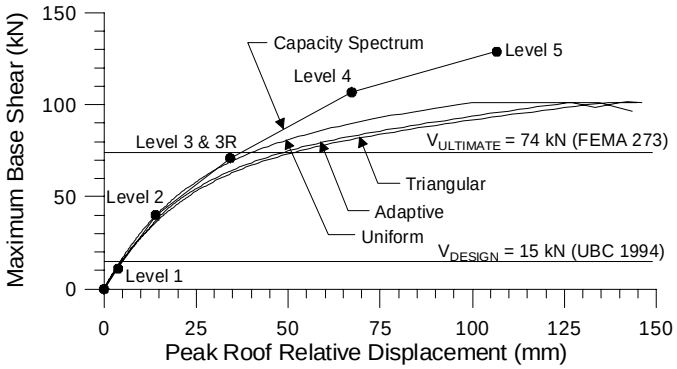

Figure 9: Experimental capacity spectrum and SAWS pushover predictions.

MODEL APPLICATIONS

Performance assessment and design procedures that are currently being developed often require multiple structural analyzes to be conducted. Obviously, with these methodologies, the computational efficiency of the analysis models becomes important. The SAWS computer program was developed with the intention of minimizing computational overhead in performing a structural analysis. Consequently, this analysis program is well suited for implementation with these approaches. Two example applications are briefly presented here. First, Fig. 10a shows the variability in response of the Phase 9 test structure to a suite of 20 earthquake records, scaled to match the NEHRP design spectrum [7]. In conjunction with this example, the SAWS computer model could easily be coupled with reliability software to conduct a reliability assessment of the test structure. As a second example, Fig. 10b shows the results of an incremental dynamic analysis [12] using the SAWS computer model applied to the Phase 9 test structure under a scaling of the 1994 Canoga Park ground motion. In both of these examples the performance of Phase 9 test structure is evaluated against the 2% drift limit for life safety [11].

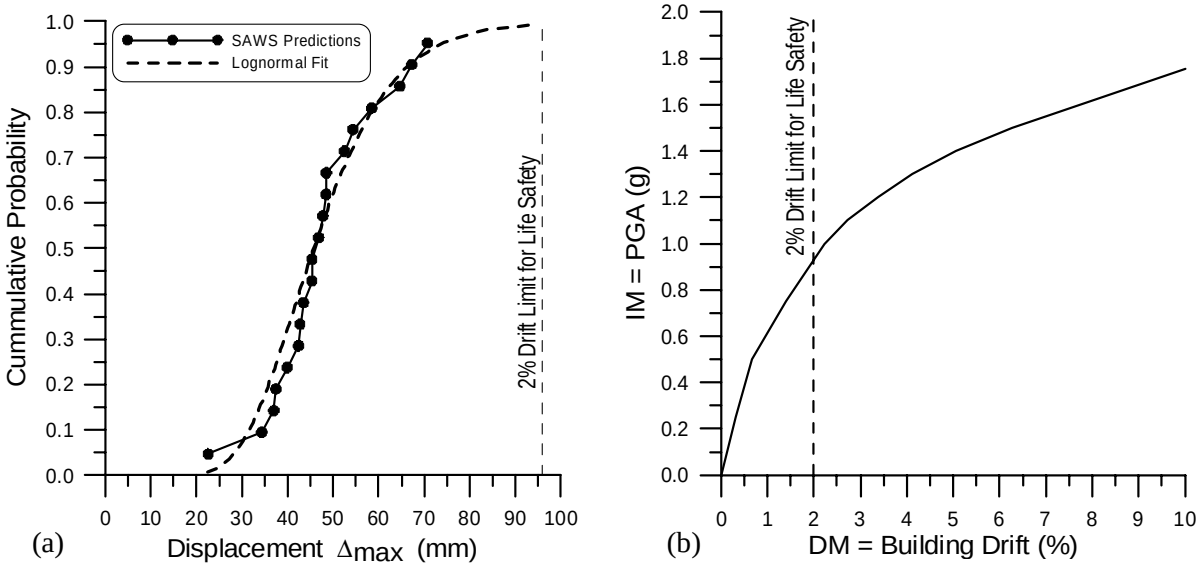

Figure 10: SAWS model applications: (a) response variability and (b) incremental dynamic analysis of the Phase 9 test structure.

CONCLUSIONS

A simple numerical model to predict the dynamic characteristics, quasi-static pushover and seismic response of woodframe buildings has been presented. This numerical model has been incorporated into the computer program SAWS - Seismic Analysis of Woodframe Structures. The predictive capabilities of the SAWS computer program have been compared with recent shake table tests performed on a full-scale two-storey woodframe house as part of the recently completed CUREE-Caltech Woodframe Project. It was shown in this study that the SAWS computer program provides reasonably accurate estimates on the dynamic characteristics, quasi-static pushover and seismic response of this test structure. Furthermore, the SAWS program requires a minimum amount of data input and provides a fast computational turn-around time to analyze a given structure. Consequently, this simple numerical model may be a useful analysis tool for the performance assessment of light-frame wood building by both practicing engineers and researchers.

ACKNOWLEDGEMENT

The work presented herein was carried out under financial support from the Consortium of Universities for Research in Earthquake Engineering (CUREE) as part of the CUREE-Caltech WoodFrame Project ("Earthquake Hazard Mitigation of Woodframe Construction") under a grant administered by the California Office of Emergency Services and funded by the Federal Emergency Management Agency. The financial support provided by these funding agencies is gratefully acknowledged. Opinions, findings conclusions and recommendations expressed in this paper are those of the writers. No liability for the information included in this paper is assumed by CUREE, California Institute of Technology, Federal Emergency Management Agency, or California Office of Emergency Services.

REFERENCES

1. Yancy CW, Cheok GS, Sadek F, Mohraz B. "A summary of the structural performance of single-family, wood-frame housing." Technical Report NISTIR 6224, National Institute of Standards and Technology, Gaithersburg, MD, 1998.
2. Kasal B, Leichti RJ, Itani RY. "Nonlinear finite-element model of complete light-frame wood structures." ASCE Journal of Structural Engineering 1994; 120(1): 100-119.
3. Folz B, Filiatrault A. "SAWS - Version 1.0: a computer program for seismic analysis of woodframe buildings." Report No. SSRP – 2001/09, Structural Systems Research Project, Department of Structural Engineering, University of California, San Diego, La Jolla, CA.
4. Philips TL, Itani, RY, McLean DI. (1993). "Lateral load sharing by diaphragms in wood-frame buildings." ASCE Journal of Structural Engineering 1993; 119(5): 1556-1571.
5. Folz B, Filiatrault A. "Cyclic analysis of wood shear walls." ASCE Journal of Structural Engineering 2001; 127(4): 433-441.
6. Folz B, Filiatrault A. "CASHEW - Version 1.1: a computer program for cyclic analysis of wood shear walls." CUREE Publication No. W-08, Richmond, CA, 2001.
7. Krawinkler H, Parisi F, Ibarra L, Ayoub A, Medina R. "Development of a testing protocol for wood frame structures." CUREE Publication No. W-02, Richmond, CA, 2000.
8. Durham JP. "Seismic response of wood shearwalls with oversized oriented strand board panels." M.A.Sc. thesis, University of British Columbia, Vancouver, Canada, 1998.
9. Fischer D, Filiatrault A, Folz B, Uang C-M, Seible F. "Shake table tests of a two-story house," CUREE Publication No. W-06, Richmond, CA, 2001.
10. International Conference of Building Officials: "Uniform Building Code 1994", Whittier, CA.
11. FEMA-273: "NEHRP Guidelines for the seismic rehabilitation of buildings," Federal Emergency Management Agency, Publication Distribution Facility, Washington, DC, 1997.
12. Vamvatsikos D, Cornell CA. "Incremental dynamic analysis." Earthquake Engineering and Structural Dynamics 2002; 31(3): 491-514.